CHAPTER 34
ENGINEERING PROPERTIES OF METALS

James E. Stallmeyer

INTRODUCTION

The design of equipment to withstand shock and vibration requires (1) a determination of the loads and resultant stresses acting on the equipment, and (2) the selection of a suitable material. The loads and stresses may be determined from an appropriate model of the equipment as described in Chap. 41. This chapter describes some of the considerations required to adapt the results from the model analysis to the selection of suitable materials, including such engineering properties as the stress-strain properties of metals and metal fatigue.

The selection of an appropriate material often involves an evaluation of the types of stress condition to which the equipment will be subjected. If a small number of severe stresses constitute the most critical situation, the most important consideration is to design the equipment for adequate strength. For equipment that will be subjected to sustained vibration or a large number of repeated applications of a load, fatigue strength is likely to be the critical design parameter. The relative importance of these types of loading must be determined for each application.

When strength is the primary design factor, an appropriate balance between stress and ductility is the most important consideration. Analytical models generally indicate the maximum stress based on linear properties of the material. If nonductile materials are used or if permanent deformation cannot be tolerated, the equipment must be designed in such a way that the stress does not exceed the elastic limit of the material. In some cases, permanent deformation may not be acceptable because it would cause misalignment of parts whose proper operation depends on accurate alignment. In other cases, permanent deformation of some structural members may be acceptable. Several empirical procedures have been developed for these cases.

One procedure, for members subjected to bending, is to permit some predetermined percentage of the cross section to yield. Ductility of the material is required for this procedure. The permanent deformation of the member, after the load has been removed, will be less than the maximum deflection because the core of an elastic material tends to restore the member to its original shape. This procedure is not

easily adapted to members subjected to loading other than bending. Another procedure establishes a maximum allowable stress equal to the yield point plus some incremental percentage of the difference between the yield point and the ultimate strength of the material. As the incremental percentage increases, the magnitude of permanent deformation increases. Consequently, the magnitude of the incremental percentage will depend upon the function of the particular member and the ability to make adjustments or repairs. For bolts which are inaccessible for retightening, the increment is generally zero. In cases where dimensional stability is important, but some yielding can be tolerated, only a small percentage increment may be permissible. When significant yielding can be tolerated, the increment may be as much as 50 percent. For bearing surfaces or where permanent deformation is permissible, the ultimate strength of the material may be used for design.

Design of equipment subject to vibration or repeated load applications requires a more detailed evaluation of the stress versus time response for the life of the structure. Three fatigue analysis procedures are available: the *stress-life method,* the *strain-life method,* and the *fracture-mechanics method.* Which of the three procedures is applicable will depend on the stress-time history. Knowledge of all three methods allows the engineer to choose the most appropriate method for the specific application.

STRESS-STRAIN PROPERTIES

STATIC PROPERTIES

The important static properties are yield strength, ultimate tensile strength, elongation at failure, and reduction of area. A standard tensile test specimen, defined by ASTM Specification A370,[1] is used to evaluate these properties. The rate of loading and the procedure for evaluation of properties are defined in the specification. Under dynamic loading the yield strength and the ultimate strength depend upon the strain rate, which in turn depends upon the geometry of the structure and the type of loading. Dynamic properties are not standardized easily. There is little information about these properties for the wide range of available metals.

The standard tensile test provides a plot of stress versus strain from which many of the mechanical properties may be obtained. A typical stress-strain curve is presented in Fig. 34.1. For materials which are linearly elastic, the elongation e is directly proportional to the length of the test bar l and the stress σ. The proportionality constant is called the modulus of elasticity E. The plot of stress versus strain usually deviates from linear behavior at the *proportional limit,* which depends on the sensitivity of the instrumentation. Most metals can be stressed slightly higher than the proportional limit without showing permanent deformation upon removal of the load. This point is referred to as the *elastic limit.* Mild steels exhibit a distinct *yield point,* at which permanent deformation

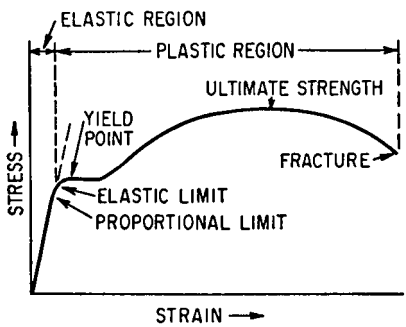

FIGURE 34.1 Typical stress-strain diagram for a metal with a yield point.

begins suddenly and continues with no increase in stress. For materials which exhibit a nonlinear stress-strain relationship, the term *yield strength* is generally used. The yield strength of a material is that stress which produces, on unloading, a permanent strain of 0.002 in./in. (0.2 percent).

Beyond the yield strength, large permanent deformations occur at a reduced modulus, the *strain-hardening modulus.* The strain-hardening modulus decreases at increasing loads until the cross-sectional area of the test bar begins to decrease, *necking,* at the ultimate load. Beyond this point further extension takes place with decreasing force. This ability of the material to flow without immediate rupture is called *ductility,* which is defined as the percent reduction of cross-sectional area measured at the section of fracture. Another measure of ductility is the percent elongation of the gage length. This value depends on the shape and size of the specimen and the gage length.

Other static properties of materials find application in the design of equipment to withstand shock and vibration. The *modulus of rigidity G* is the ratio of shear stress to shear strain; it may be determined from the torsional stiffness of a thin-walled tube of the material. The value of G for steel is 12×10^6 lb/in.^{2}. Poisson's ratio ν is the ratio of the lateral unit strain to the normal unit strain in the elastic range of the material. This ratio evaluates the deformation of a material that occurs perpendicular to the direction of application of load. The value of ν for steel is 0.3. More complete data on materials and their properties as used in machine and equipment design are compiled in available references.[2–4] Values of the static properties of typical engineering materials are given in Tables 34.1 to 34.3. (All values of σ, G, and E in these and later tables may be converted to SI units by MPa = 145 lb/in.^{2}.)

TABLE 34.1 Mechanical Properties of Typical Cast Irons (*A. Vallance and V. Doughtie.*[2])

Material	Ultimate strength: Tension, lb/in.^{2}, σ_u†	Ultimate strength: Compression, lb/in.^{2}, σ_u	Endurance limit in reversed bending lb/in.^{2}, σ_e	Brinell hardness number	Modulus of elasticity: Tension and compression, lb/in.^{2}, E	Modulus of elasticity: Shear lb/in.^{2}, G	Elongation in 2 in., %
Gray, ordinary	18,000	80,000	9,000	100–150	10–12,000,000	4,000,000	0–1
Gray, good*	24,000 16,000	100,000	12,000	100–150	12,000,000	4,800,000	0–1
Gray, high grade	30,000	120,000	15,000	100–150	14,000,000	5,600,000	0–1
Malleable, S.A.E. 32510	50,000	120,000	25,000	100–145	23,000,000	9,200,000	10
Nickel alloys:							
Ni-0.75, C-3.40, Si-1.75, Mn-0.55*	32,000 24,000	120,000	16,000	200 175	15,000,000	6,000,000	1–2
Ni-2.00, C-3.00, Si-1.10, Mn-0.80*	40,000 31,000	155,000	20,000	220 200	20,000,000	8,000,000	1–2
Nickel-chromium alloys:							
Ni-0.75, Cr-0.30, C-3.40, Si-1.90, Mn-0.65	32,000	125,000	16,000	200	15,000,000	6,000,000	1–2
Ni-2.75, Cr-0.80, C-3.00, Si-1.25, Mn -0.60	45,000	160,000	22,000	300	20,000,000	8,000,000	1–2

* Upper figures refer to arbitration test bars. Lower figures refer to the center of 4-in. round specimens.

† *Flexure:* For cast irons in bending, the modulus of rupture may be taken as 1.75 σ_u (tension) for circular sections, 1.50 σ_u for rectangular sections and 1.25 σ_u for I and T sections.

TABLE 34.2 Mechanical Properties of Typical Carbon Steels (*A. Vallance and V. Doughtie.*[2])

Material	Ultimate strength: Tension, lb/in.^{2}, σ_u	Ultimate strength: Shear, lb/in.^{2}, σ_u	Yield strength: Tension and compression, lb/in.^{2}, σ_y	Yield strength: Shear, lb/in.^{2}, σ_y	Endurance limit in reversed bending lb/in.^{2}, σ_e	Brinell hardness number	Modulus of elasticity: Tension and compression, lb/in.^{2}, E	Modulus of elasticity: Shear, lb/in.^{2}, G	Elongation 2 in., %
Wrought iron	48,000	50,000	27,000	30,000	25,000	100	28,000,000	11,200,000	30–40
Cast steel:									
Soft	60,000	42,000	27,000	16,000	26,000	110	30,000,000	12,000,000	22
Medium	70,000	49,000	31,500	19,000	30,000	120	30,000,000	12,000,000	18
Hard	80,000	56,000	36,000	21,000	34,000	130	30,000,000	12,000,000	15
SAE 1025:									
Annealed	67,000	41,000	34,000	20,000	29,000	120	30,000,000	12,000,000	26
Water-quenched*	78,000	55,000	41,000	24,000	43,000	159	30,000,000	12,000,000	35
	90,000	63,000	58,000	34,000	50,000	183			27
SAE 1045:									
Annealed	85,000	60,000	45,000	26,000	42,000	140	30,000,000	12,000,000	20
Water-quenched*	95,000	67,000	60,000	35,000	53,000	197	30,000,000	12,000,000	28
	120,000	84,000	90,000	52,000	67,000	248			15
Oil-quenched*	96,000	67,000	62,000	35,000	53,000	192	30,000,000	12,000,000	22
	115,000	80,000	80,000	45,000	65,000	235			16
SAE 1095:									
Annealed	110,000	75,000	55,000	33,000	52,000	200	30,000,000	12,000,000	20
Oil-quenched*	130,000	85,000	66,000	39,000	68,000	300	30,000,000	11,500,000	16
	188,000	120,000	130,000	75,000	100,000	380			10

* Upper figures: steel quenched and drawn to 1300°F. Lower figures: steel quenched and drawn to 800°F. Values for intermediate drawing temperatures may be approximated by direct interpolation.

TEMPERATURE AND STRAIN-RATE EFFECTS

The static properties of most engineering materials depend upon the testing temperature. As the testing temperature is increased above room temperature, the yield point, ultimate strength, and modulus of elasticity decrease. For example, the yield point of structural carbon steel is about 90 percent of the room-temperature value at 400°F (204°C), 60 percent at 800°F (427°C), 50 percent at 1000°F (538°C), 20 percent at 1300°F (704°C), and 10 percent at 1600°F (871°C). The corresponding changes for ultimate strength are 100 percent of the room-temperature value at 400°F, 85 percent at 800°F, 50 percent at 1000°F, 15 percent at 1300°F, and 10 percent at 1600°F. Changes in the modulus of elasticity are 95 percent of the room-temperature value at 400°F, 85 percent at 800°F, 80 percent at 1000°F, 70 percent at 1300°F, and 50 percent at 1600°F. As a result of these changes in properties, the ductility is increased significantly.

When materials are tested in temperature ranges where creep of the material occurs, the creep strains will contribute to the inelastic deformation. The magnitude of the creep strain increases as the speed of the test decreases. Consequently, tests at elevated temperatures should be conducted at a constant strain rate, and the value

TABLE 34.3 Mechanical Properties of Copper-Zinc Alloys (Brass)
(*A. Vallance and V. Doughtie*[2])

Type of material	Ultimate strength: Tension, lb/in.^{2}, σ_u	Yield strength: Tension, lb/in.^{2}, σ_e	Endurance limit, lb/in.^{2}, σ_e	Brinell hardness number	Modulus of elasticity: Tension and compression, lb/in.^{2}, E	Elongation in 2 in., %
Commercial bronze (90 Cu, 10 Zn):						
Rolled, hard	65,000	63,000	18,000	107	15,000,000	18
Rolled, soft	35,000	11,000	12,000	52	15,000,000	56
Forged, cold	40,000–65,000	25,000–61,000	12,000–16,000	62–102	15,000,000	55–20
Red brass (85 Cu, 15 Zn):						
Rolled, hard	75,000	72,000	20,000	126	15,000,000	18
Rolled, soft	37,000	14,000	14,000	54	15,000,000	55
Forged, cold	42,000–62,000	22,000–54,000	14,000–18,000	63–120	15,000,000	47–20
Low brass (80 Cu, 20 Zn):						
Rolled, hard	75,000	59,000	22,000	130	15,000,000	18
Rolled, soft	44,000	12,000	15,000	56	15,000,000	65
Forged, cold	47,000–80,000	20,000–65,000		63–133	15,000,000	30–15
Spring brass (75 Cu, 25 Zn):						
Hard	84,000	64,000	21,000	107*	14,000,000	5
Soft	45,000	17,000	17,000	57*	18,000,000	58
Cartridge brass (70 Cu, 30 Zn):						
Rolled, hard	100,000	75,000	22,000	154	15,000,000	14
Rolled, soft	48,000	30,000	17,000	70	15,000,000	55
Deep-drawing brass (68 Cu, 32 Zn):						
Strip, hard	85,000	79,000	21,000	106*	15,000,000	3
Strip, soft	45,000	11,000	17,000	13*	15,000,000	55
Muntz metal (60 Cu, 40 Zn):						
Rolled, hard	80,000	66,000	25,000	151	15,000,000	20
Rolled, soft	52,000	22,000	21,000	82	15,000,000	48
Tobin bronze (60 Cu, 39.25 Zn, 0.75 Sn):						
Hard	63,000	35,000	21,000	165	15,000,000	35
Soft	56,000	22,000		90	15,000,000	45
Manganese bronze (58 Cu, 40 Zn):						
Hard	75,000	45,000	20,000	110	15,000,000	20
Soft	60,000	30,000	16,000	90	15,000,000	30

* Rockwell hardness F.

used should be reported along with the results. Creep strains may be significant at room temperature for materials with low melting temperatures.

The yield strength and the ultimate strength of certain metals, as well as the entire stress level of the stress-strain curve, are increased when the rate of deformation is increased. Figure 34.2 presents information on the static and dynamic values of the ultimate strength of several metals when the dynamic strength is determined at impact velocities of 200 to 2500 ft/sec (60 to 76 m/s).[5] The influence of strain rate

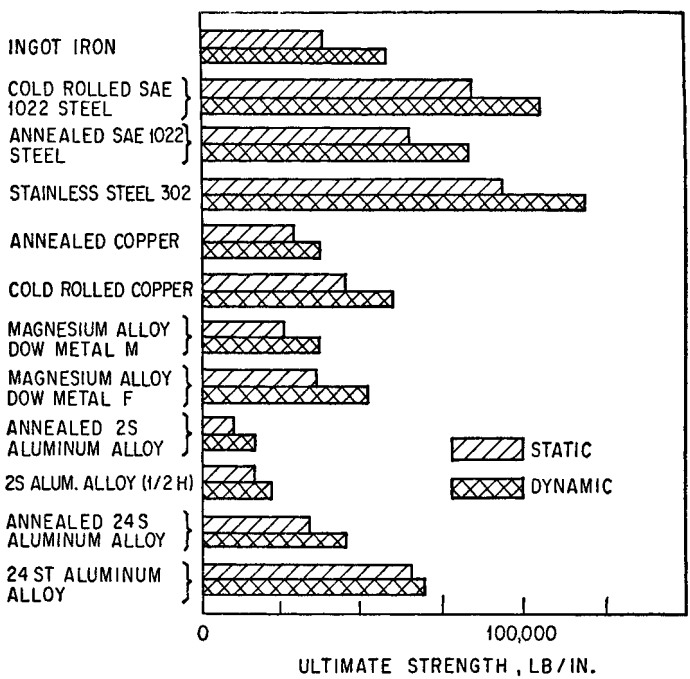

FIGURE 34.2 Static and dynamic values of the ultimate strength of several metals when the dynamic strengths were obtained at impact velocities of 200 to 250 ft/sec. (*D. S. Clark and D. S. Wood.*[5])

on the tensile properties of mild steel at room temperature is shown in Fig. 34.3. The marked difference between the yield stress and ultimate stress at low rates of strain disappears at high rates of strain.[6] Figure 34.3 also shows that the ultimate stress remains practically unchanged for strain rates below 1 in./in./sec. In this limited range the stress-strain curve of most engineering metals is not raised appreciably.[7] Mild steel is an exception in which the yield stress in influenced markedly by strain rate in the range from 0 to 1 in./in./sec.

Although the yield strength and ultimate strength of mild steel show an increase as the rate of strain increases, as illustrated in Fig. 34.3, this effect is of very limited significance in the design of equipment to withstand shock and vibration. In general, a strain rate great enough to cause a significant increase in strength occurs only

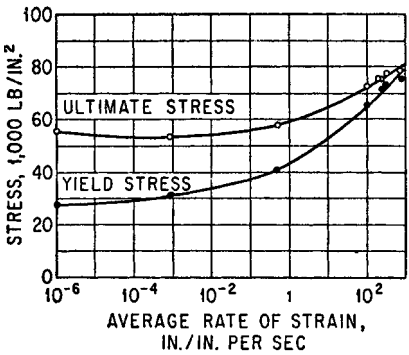

FIGURE 34.3 Effect of strain rate on mechanical properties of mild steel. (*M. J. Manjoine.*[6])

closely adjacent to a source of shock, as at the point of impact of a projectile on armor plate. Equipment seldom is subjected to shock of this nature. In a typical installation, the structure interposed between the equipment and the source of shock is unable to transmit large forces suddenly enough to cause high strain rates at the equipment. Furthermore, the response of a structure to a shock is oscillatory; maximum strain rate occurs at zero strain, and vice versa. The data of Fig. 34.3 represent conditions where maximum stress and maximum rate of strain occur simultaneously; thus, they do not apply directly to the design of shock-resistant equipment. The use of statically determined yield strength and ultimate strength for design purposes is a conservative (but not overly conservative) practice.

TOUGHNESS AND DUCTILITY

It is useful to evaluate the total energy needed to fracture a test bar under tension; this energy is a measure of the *toughness* of the material. The area under the typical stress-strain diagram shown in Fig. 34.1 gives an approximate measure of the fracture energy per unit volume of material. However, the true fracture energy depends upon the true stress and true strain characteristics, which take into account the nonuniform strain resulting from the reduction of area upon necking of the test bar. Calculated values of the fracture energy for various metals are given in Table 34.4. Tough materials (e.g., wrought iron and low- or medium-carbon steel) exhibit high unit elongation and are considered to be ductile. By contrast, cast iron exhibits practically no elongation and is considered to be brittle. If only the elastic strain energy up to the proportional limit is included, the resulting stored energy per unit volume is called the *modulus of resilience.* Values of this property are also given in Table 34.4.

CRITICAL STRAIN VELOCITY

When a large load is applied to a structure very suddenly, failure of the structure may occur with a relatively small overall elongation. This has been interpreted as a *brittle fracture,* and it has been said that a material loses its ductility at high strain rates. However, an examination of the failure shows normal ductility (necking) in a region close to the application of load. Large stresses are developed in this region by the inertia of the material remote from the application of the load, and failure occurs before the plastic stress waves are transmitted away from the point of load application. This effect is important only where loads are applied very suddenly, as in a direct hit by a projectile on armor plate. In general, equipment is mounted upon structures that are protected from direct hits; the resilience of such structures prevents a sufficiently rapid application of load for the above effect to be of significance in the design of equipment.

TABLE 34.4 Fracture Energy or Toughness of Different Materials (*J. M. Lessells.*[8])

Material	Condition	Yield strength, lb/in.^{2}, σ_y	Tensile strength, lb/in.^{2}, σ_u	Unit elongation, in./in., ξ	Toughness or fracture energy, in.-lb/in.^{3}	Modulus of resilience, in.-lb/in.^{3}
Wrought iron	As received	24,000	47,000	0.50	17,700	7
Steel (0.13% C)	As received	26,000	54,000	0.44	17,600	11
Steel (0.25% C)	As received	44,000	76,000	0.36	21,600	24
Steel (0.53% C)	Oil-quenched and drawn	86,000	134,000	0.11	12,000	100
Steel (1.2% C)	Oil-quenched and drawn	130,000	180,000	0.09	10,800	280
Steel (spring)	Oil-quenched and drawn	140,000	220,000	0.03	4,400	320
Cast iron	As received	. . .	20,000	0.005	70	1
Nickel cast iron	As received	20,000	50,000	0.10	3,500	9
Rolled bronze	As received	40,000	65,000	0.20	10,500	60
Duralumin	Forged and heat-treated	30,000	52,000	0.25	10,200	17

DELAYED INITIATION OF YIELD

Sudden application of load may not immediately result in yielding of a structure made of ductile material. Rather, yielding may occur after some time delay. This delay in initiation of yield is a function of the material, stress level, rate of load application, and temperature. Consequently, a material may be stressed substantially above its yield strength for a short period of time without yielding. For mild steel at room temperature, the delay time is of the order of 0.001 sec. For repeated applications of load, the material has a memory; i.e., the durations of load are additive to determine the time of yielding. Equipment subjected to shock or vibration experiences an oscillatory stress pattern wherein the higher stresses occur repeatedly. The durations of these stresses quickly add up to a time greater than the delay time for common materials; thus, the effect is of little significance in the design of equipment to withstand shock and vibration.

FATIGUE

The strength properties discussed up to this point are important to ensure structural integrity in the event of a single application of severe loading. Most structures, however, will be subjected to many applications of loads that may be considerably below the static-load capacity of the member or structure. Under such circumstances, localized permanent changes in the material may lead to the initiation of small cracks, which propagate under subsequent applications of cyclic load. Cracks may initiate from crystal imperfections, dislocations, microcracks, lack of penetration, porosity, etc. The rate of propagation increases as the crack grows in size. If the crack becomes sufficiently large, the static load capacity of the member may be exceeded, resulting in a ductile failure. If a critical crack length is reached, the member may fail by brittle fracture at some stress significantly below the ultimate strength of the material. The critical crack length is a function of stress level, temperature, and material properties. A comprehensive discussion of the factors which contribute to brittle fracture can be found in Ref. 11.

Fatigue behavior is affected by a variety of factors. Some of the more important parameters which influence the fatigue response are the properties of the material, rate of cyclic loading, stress magnitude, residual stresses, size effect, geometry, and prior strain history. The basic parameters in fatigue tests are the stress level and the number of cycles to failure. The effects of other parameters are studied by evaluating the changes which occur in the relationship between stress and cycles to failure as these parameters are introduced.

The tensile properties of a material serve as a guide in selecting materials. They are used quantitatively to proportion members to resist static loading. There is no equivalent set of fatigue properties available to the designer whose structure must resist cyclic loading. Fatigue theories attempt to relate stress-strain properties to fatigue behavior, but complexities which arise during fatigue have thwarted these attempts. The design of equipment to resist repetitive load cycles is based on empirical data or on the application of crack propagation laws.

Fatigue tests are conducted by subjecting a test specimen to a stress pattern in which the stress varies with time. The test specimen may be subjected to alternating bending stress, as in the case of the rotating beam specimen, or to alternating axial stress. Most fatigue tests are conducted under conditions in which the stress varies sinusoidally with time. However, the use of servo-controlled hydraulic testing machines permits the variation of stress with time to follow any desired pattern. Tests may be carried out under alternating tension and compression, alternating torsion, alternating tension superimposed upon cyclic alternating tension, and many others.

Most fatigue data available in the literature have been obtained from tests which involve cycling between maximum and minimum stress levels of constant value. These are referred to as *constant-amplitude tests.* Parameters of interest are the *stress range,* $\Delta\sigma$; and the average of the maximum and minimum stress in the stress range, σ_m. One-half the stress range is called the *stress amplitude,* σ_a. The mathematical formulations for these basic definitions are

$$\Delta\sigma = \sigma_{max} - \sigma_{min} \tag{34.1}$$

$$\sigma_m = \frac{\sigma_{max} + \sigma_{min}}{2} \tag{34.2}$$

$$\sigma_a = \frac{\Delta\sigma}{2} \tag{34.3}$$

The ratio $\sigma_{max}/\sigma_{min}$ is referred to as the *stress ratio, R,* and the ratio between σ_a and σ_m is referred to as the *amplitude ratio, A. Completely reversed stressing* describes the case in which $\sigma_m = 0$, for which $R = -1$. The term *zero-to-tension stressing* is applied to the case in which $\sigma_{min} = 0$, and hence $R = 0$.

Most fatigue data are presented in the form of a stress (or strain) parameter versus the cycles to failure (*S-N* curves) obtained in laboratory tests. A schematic *S-N* curve is shown in Fig. 34.4. The stress parameter in this plot is the stress range, $\Delta\sigma$. The maximum stress in the test specimen is also used for this parameter.

Cycles to failure reported in the fatigue literature depend upon the definition of failure used in the particular investigation. Failure may be defined as the first appearance of an observable crack. A crack of a specific length may also be used as a failure criterion. Finally, the inability to resist the applied load without significant crack extension or corresponding load relaxation in a constant-amplitude deformation test may be used to denote failure.

Figure 34.4 also contains plots which represent the portion of the total life contributed by the crack initiation phase and by the crack propagation phase. At high levels of stress the major portion of the life consists of crack propagation, while at

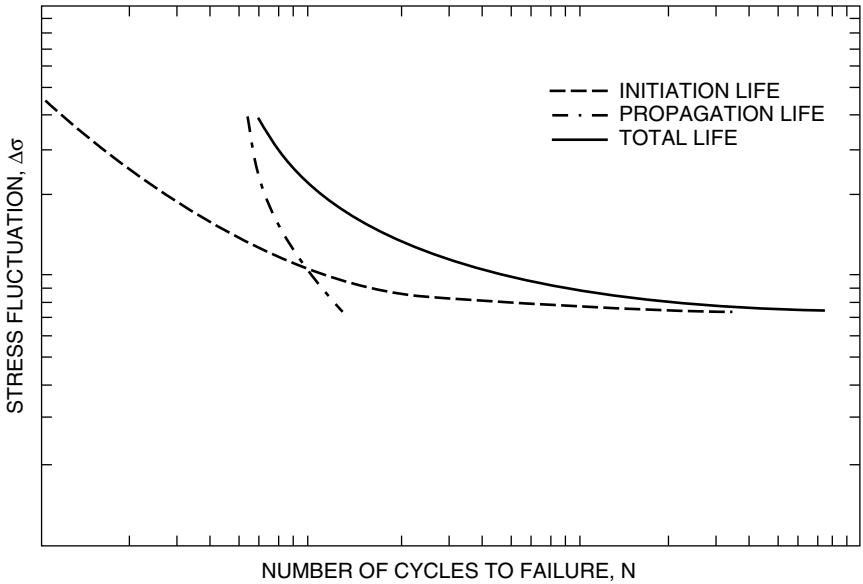

FIGURE 34.4 Schematic *S-N* curve divided into initiation and propagation components. (*J. M. Barsom and J. T. Rolfe, p. 251, Ref. 11.*)

low stress levels crack initiation constitutes the major portion of the life. Design procedures for structural components which may have surface irregularities different from those of the test specimens or which may contain cracklike discontinuities or flaws must take this difference in behavior into account.

The lowest value of stress or stress amplitude for which the crack propagation is so small that the number of cycles to failure appears to be infinite, *run-out,* is commonly referred to as the *endurance limit.* Representative values of the endurance limit for a variety of materials are presented in Tables 34.5 and 34.6. The effects of geometry and corrosive environment on the relationship between fatigue strength and ultimate strength of steels are shown in Fig. 34.5.

Three design approaches are presented in the following sections. The stress-life method was the first approach employed and has been the standard method for many years. It is still widely used in applications in which the applied stress is within the elastic range. It does not work well where the applied strains have a significant plastic component, *low-cycle fatigue.* A strain-life approach is more appropriate in this case. A more recent development in the evaluation of fatigue life incorporates the concepts of fracture mechanics to analyze the crack growth from some initial flaw size as cyclic stresses are applied. In this approach, failure may be defined as the development of a crack of some specific dimension. Detailed discussions of the different methods are given in Refs. 10 and 11.

STRESS-LIFE METHOD

The first procedure used to design structural components utilizes a design fatigue curve which characterizes the basic unnotched fatigue properties of the material and

TABLE 34.5 Tensile and Fatigue Properties of Steels (*J. M. Lessells.*[8])

Material	State	Yield strength, lb/in.^{2}, σ_y	Tensile strength, lb/in.^{2}, σ_u	Elongation, %	Reduction of area, %	Endurance limit, lb/in.^{2}, σ_e	Ratio σ_e/σ_u
0.02% C	As received	19,000	42,400	48.3	76.2	26,000	0.61
Wrought iron	As received	29,600	47,000	35.0	29.0	23,000	0.49
0.24% C	As received	38,000	60,500	39.0	64.0	25,600	0.425
0.24% C	Water-quenched and drawn	45,600	67,000	38.0	71.0	30,200	0.45
0.37% C	Normalized	34,900	71,900	29.4	53.5	33,000	0.46
0.37% C	Water-quenched and drawn	63,100	94,200	25.0	63.0	45,000	0.476
0.52% C	Normalized	47,600	98,000	24.4	41.7	42,000	0.43
0.52% C	Water-quenched and drawn	84,300	111,400	21.9	56.6	55,000	0.48
0.93% C	Normalized	33,400	84,100	24.8	37.2	30,500	0.36
0.93% C	Oil-quenched and drawn	67,600	115,000	23.0	39.6	56,000	0.487
1.2% C	Normalized	60,700	116,900	7.9	11.6	50,000	0.43
1.2% C	Oil-quenched and drawn	130,000	180,000	9.0	15.2	92,000	0.51
0.31% C, 3.35% Ni	Normalized	53,500	104,000	23.0	45.0	49,500	0.47
0.31% C, 3.35% Ni	Oil-quenched and drawn	130,000	154,000	17.0	49.0	63,500	0.41
0.24% C, 3.3% Ni, 0.87% Cr	Oil-quenched and drawn	128,000	138,000	18.2	61.8	68,000	0.49

a fatigue-strength reduction factor. Parameters characteristic of the specific component which make it more susceptible to fatigue failure than the unnotched specimen are reflected in the strength-reduction factor. Early applications of this method were based on the results of rotating bending tests. The application of such tests, in which mirror-polished specimens were subjected to reversed bending, requires consideration of a number of factors which present themselves in design situations. Among these factors are size, type of loading, surface finish, surface treatments, temperature, and environment.

In the rotating beam test, a relatively small volume of material is subjected to the maximum stress. For larger rotating beam specimens, the volume of material is greater, and therefore there will be a greater probability of initiating a fatigue crack. Similarly, an axially loaded specimen which has no gradient will exhibit an endurance limit smaller than that obtained from the rotating beam test. Surface finish will have a similar effect. Surface finish is more significant for higher-strength steels. At shorter lives (high stress levels), surface finish has a smaller effect on the fatigue life. Surface treatment, temperature, and environment have similar effects.

The effect of mean stress on fatigue life is conveniently represented in the form of a modified Goodman fatigue diagram (Fig. 34.6). In this figure, the ordinate is the maximum stress, and the abscissa is the minimum stress. Radial lines indicate the stress ratio. The curves n_1, n_2, etc., represent failure at various lives.

Many design specifications[12–15] contain provisions for repeated loadings based on laboratory tests. In these specifications, fabricated details are categorized for

TABLE 34.6 Tensile and Fatigue Properties of Nonferrous Metals (*J. M. Lessells.*[8])

Material	State	Tensile strength, lb/in.^{2}, σ_u	Endurance limit or fatigue strength, lb/in.^{2}, σ_e	N_1,* millions of cycles	N_2† millions of cycles	Ratio σ_e/σ_u
Aluminum		22,600	10,500	100	6	0.46
Duralumin	Rolled	51,000	14,000	400	>400	0.27
Duralumin	Annealed	25,200	10,000	200	>200	0.40
Duralumin	Tempered	51,300	12,000	400	4½	0.24
Magnesium	Extruded	32,500	8,000	200	2	0.25
Magnesium alloy (4% Al)		35,200	12,000	600	½	0.34
Magnesium alloy (4% Al, 0.25% Mn)		39,000	15,000	100	1	0.38
Magnesium alloy (6.5% Al)		41,200	13,000	600	½	0.31
Magnesium alloy (6.5% Al, 0.25% Mn)		44,500	15,000	100	½	0.34
Magnesium alloy (10% Cu)		39,000	12,000	600	½	0.31
Electron metal		36,600	17,000	200	30	0.47
Copper	Annealed	32,400	10,000	500	20	0.31
Copper	Cold-drawn	56,200	10,000	500	>500	0.18
Brass (60–40)	Annealed	54,200	22,000	500	>500	0.44
Brass (60–40)	Cold-drawn	97,000	26,000	500	50	0.27
Naval brass		68,400	22,000	300	10	0.32
Aluminum bronze (10% Al)	As cast	59,200	23,000	60	3	0.39
Aluminum bronze (10% Al)	Heat-treated	77,800	27,000	40	1	0.35
Bronze (5% Sn)	Annealed	45,600	23,000	1000	10	0.50
Bronze (5% Sn)	Cold-drawn	85,000	27,000	500	50	0.32
Manganese bronze	As cast	70,000	17,000	150	20	0.24
Nickel	Annealed	70,000	28,000	100	50	0.40
Monel metal	Hot-rolled	90,000	32,000	450	>450	0.36

* N_1 = cycles on which σ_e is based.
† N_2 = cycles at which σ-N curve becomes and remains horizontal.

design purposes and fatigue-strength stress ranges are given for different fatigue lives.

The following procedure[16] has been used to determine an allowable fatigue design stress range, S_R. Four different loading histograms, shown in Fig. 34.7, were used to describe the frequency distribution of the ratio of the cyclic stress range to the maximum cyclic stress range. The four conditions are defined in Table 34.7; the first three represent beta-distribution probability density functions that have shape factors q and r as shown. The allowable fatigue design stress range S_R may be determined from

$$S_R = S_r R_F C_L \tag{34.4}$$

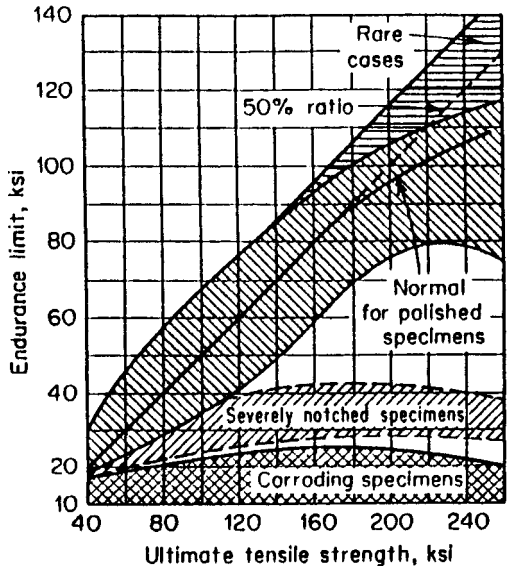

FIGURE 34.5 Relationship between the fatigue limit and ultimate tensile strength of various steels. (*Battelle Memorial Institute.*[9])

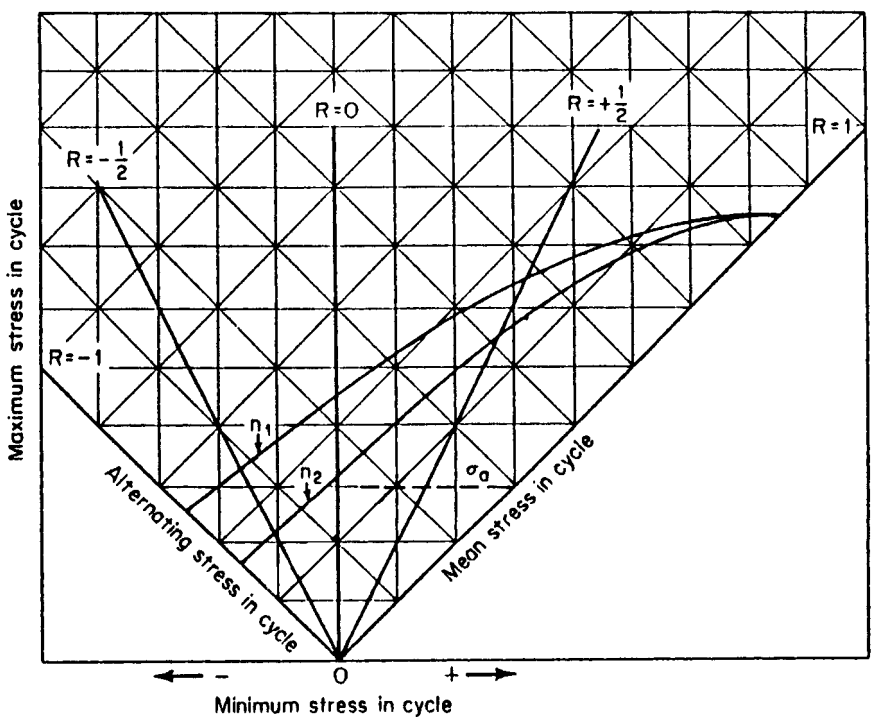

FIGURE 34.6 Modified Goodman diagram for various lives and stress ranges.

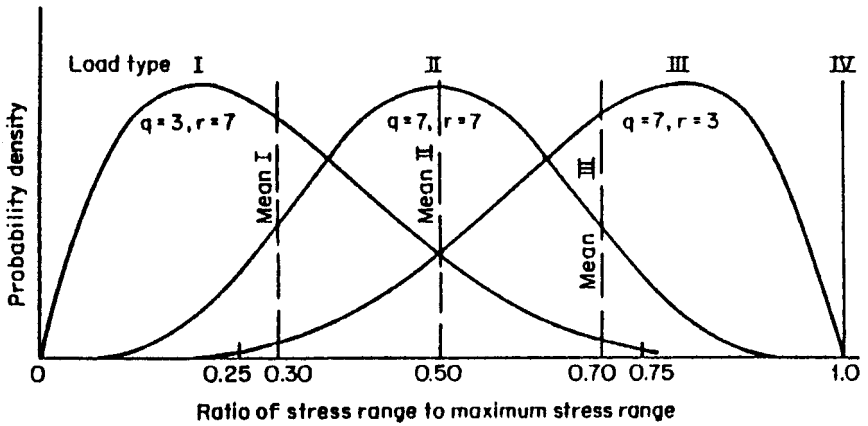

FIGURE 34.7 Loading frequency distributions. (*W. H. Munse and S. T. Rolfe, Sect. 4 of Ref. 16.*)

TABLE 34.7 Random Loading Coefficients C_L

Type	Load description (see Fig. 34.7)	Coefficient C_L
I	Primarily light loading cycles: mean range of stress 030% of maximum ($q = 3, r = 7$)	2.75
II	Medium loading cycles: mean range of stress 50% of maximum ($q = 7, r = 7$)	1.85
III	Primarily heavy loading cycles: mean range of stress 70% of maximum ($q = 7, r = 3$)	1.35
IV	Constant loading cycles: stress range constant and equal to 100% of maximum	1.00

TABLE 34.8 Reliability Factors R_F

Level of reliability	Structural importance of detail	Reliability factor R_F
90%	Secondary details for which fatigue cracking is of little structural significance	0.67
95%	Major structural details for which fatigue cracking is important: members in redundant structures	0.60
99%	Major structural details in fracture-critical members where fatigue cracking is critical	0.45

where S_r = mean constant-cycle fatigue stress range for desired life
R_F = reliability factor based on a statistical fatigue analysis for survival, Table 34.8
C_L = loading coefficient to be selected for load type, Table 34.7

The stress-life method works quite well for the design for long-life and constant-amplitude stress histories.

STRAIN-LIFE METHOD

At high load levels, at which plastic strains are likely to occur, the response and material behavior are best modeled under strain-controlled conditions. Engineered structures almost always contain points of stress concentration which cause plastic strains to develop. The constraint imposed by the surrounding elastic material produces an essentially strain-controlled environment. For these conditions, tests under strain control are used to simulate fatigue damage at points of stress concentration. The strain-life method does not account for crack growth. Consequently, such methods may be considered initiation life estimates. For components in which the existence of a crack may be an overly conservative criterion, fracture mechanics may be employed to assess the crack propagation life from some assumed initial crack size.

Cyclic inelastic loading of a material produces a hysteresis loop. The stress range, $\Delta\sigma$, is the total height of the loop. The total width of the loop is $\Delta\epsilon$, the total strain range. The strain amplitude, ϵ_a, can be expressed by

$$\epsilon_a = \frac{\Delta\epsilon}{2} \tag{34.5}$$

and the stress amplitude, σ_a, is

$$\sigma_a = \frac{\Delta\sigma}{2} \tag{34.6}$$

The sum of the elastic and plastic strain ranges is the total strain, $\Delta\epsilon$. This may be expressed mathematically as

$$\Delta\epsilon = \Delta\epsilon_e + \Delta\epsilon_p \tag{34.7}$$

In terms of amplitudes

$$\frac{\Delta\epsilon}{2} = \frac{\Delta\epsilon_e}{2} + \frac{\Delta\epsilon_p}{2} \tag{34.8}$$

The elastic term may be replaced by $\Delta\sigma/E$ by applying Hooke's law, so that

$$\frac{\Delta\epsilon}{2} = \frac{\Delta\sigma}{2E} + \frac{\Delta\epsilon_p}{2} \tag{34.9}$$

Under repeated cycling the stress-strain response may exhibit cyclic hardening, cyclic softening, cyclic stability, or a mixed behavior (softening or hardening depending upon the stress range).

From experimental data, the following relationship between total strain range and the number of reversals to failure has been developed:

$$\frac{\Delta\epsilon}{2} = \frac{\sigma'_f}{E}(2N_f)^b + \epsilon'_f(2N_f)^c \tag{34.10}$$

where $\Delta\epsilon$ = total strain range
σ'_f = fatigue strength coefficient
$2N_f$ = reversals to failure
b = fatigue strength exponent
ϵ'_f = fatigue ductility coefficient
c = fatigue ductility exponent

The fatigue strength coefficient, σ'_f, is approximately equal to the true fracture strength. The fatigue strength exponent, b, varies between –0.05 and –0.12. The fatigue ductility coefficient, ϵ'_f, is approximately equal to the true fracture ductility. The fatigue ductility exponent, c, varies between –0.5 and –0.07. Additional discussion of these parameters and approximate formulations for the fatigue strength coefficient and the fatigue ductility coefficient are presented in Ref. 10.

Cyclic properties are generally obtained from completely reversed, constant-amplitude, strain-controlled tests. The effects of mean strain have been studied by various investigators, and modifications of Eq. (34.10) have been proposed.

This method of analysis is obviously more complicated than the stress-life approach. Notch root strains must be evaluated by application of some method of analysis. Since it is based on strain cycling of constant magnitude, it applies only in the immediate region of the notch and predicts the initiation life for a fatigue crack.

FRACTURE MECHANICS METHOD

Fracture mechanics is the study of the performance of structures with cracklike defects. The distribution of stress components at the crack tip are related to a constant called the *stress intensity factor,* characterized by the applied stress and the dimensions of the crack. In addition to the applied stress, the design process using fracture mechanics incorporates flaw size and fracture toughness properties of the material. Fracture toughness replaces strength as the relevant material property.

As noted earlier, fatigue life is divided into an initiation phase and a propagation phase. The fracture mechanics method can be used to determine the propagation life on the assumption of some initial crack or defect size. The strain-life approach may be used to determine the initiation life for an evaluation of the total fatigue life.

Fatigue crack growth under constant-amplitude cyclic loading can be represented schematically as shown in Fig. 34.8. Such data can be presented in terms of crack growth rate per cycle of loading, da/dN, and the fluctuation of the stress intensity factor, ΔK_1. The most common presentation of fatigue crack growth data is as a log-log plot of the rate of fatigue crack growth per cycle of load fluctuation, da/dN, and the fluctuation of the stress intensity factor, ΔK_1. Such a plot shows three distinct regions. At low values of ΔK, the rate of crack propagation is extremely small, essentially zero. The value of ΔK for this condition is referred to as the fatigue-threshold cyclic stress intensity factor fluctuation, ΔK_{th}, below which cracks do not propagate. There are sufficient data available to demonstrate the existence of this threshold, but more work is needed to determine the factors which affect its magnitude for use in design.

The second stage in the crack propagation versus stress intensity factor relationship represents the fatigue crack propagation behavior above ΔK_{th}. In this region the relationship can be defined as

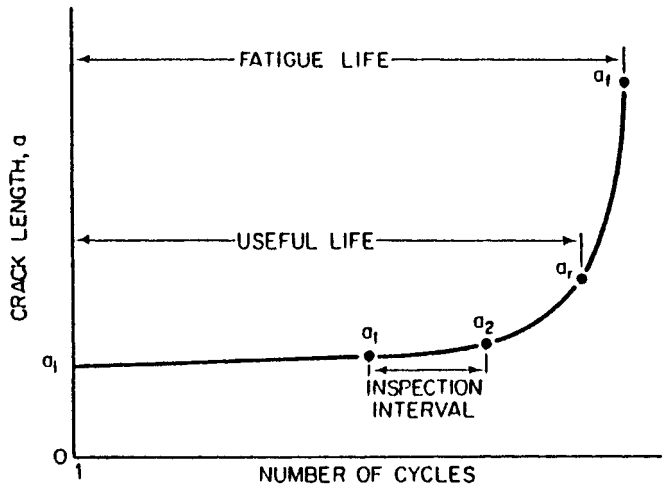

FIGURE 34.8 Schematic representation of fatigue crack growth curve under constant-amplitude loading. (*J. M. Barsom and S. T. Rolfe, p. 279, Ref. 11.*)

$$\frac{da}{dN} = A(\Delta K)^m \tag{34.11}$$

where a = crack length
N = number of cycles
ΔK = stress intensity factor range

and A and m are constants that depend on the properties of the material.

The third stage in the crack propagation versus stress intensity factor relationship shows a very rapid increase in the rate of crack propagation.

Fatigue crack propagation may be affected by the mean stress, cyclic frequency, waveform, and environment. Extensive discussion of the effect of these parameters, as well as values of A and m for different materials, is presented in Ref. 11.

Equation (34.11) can be used, with appropriate values of A and m, to analyze fatigue crack growth as a function of cyclic loading between some assumed initial crack size and some critical crack dimension assumed to represent the ultimate condition. The critical crack dimension may be chosen on the basis of the limiting static strength or on the basis of the crack size which may result in brittle fracture. The procedure requires the integration of Eq. (34.11) from an initial crack size, a_0, which corresponds to an initial value of ΔK. An increment of crack growth must be incorporated, during which stage the value of ΔK remains constant. The value of ΔK is then revised and the process is continued until the crack reaches the limiting critical dimension. An example of this procedure is presented in Ref. 11.

VARIABLE-AMPLITUDE LOADING

Most laboratory fatigue tests are conducted at constant values of maximum and minimum stress. Most structures, on the other hand, are subjected to loading cycles with variable minimum and maximum stresses over the course of their life. Proce-

dures are required to relate the behavior under constant cyclic loading obtained in laboratory tests and the variations of stress history over time which occur in an actual structure. It is also necessary to convert the complicated time-history of a real structure into some equivalent number of individual stress cycles for the evaluation of their cumulative effect.

DAMAGE RULES

Damage during the initiation phase of fatigue is difficult to assess, as it occurs on a microscopic level and is not easily observed or evaluated. During the propagation phase, damage can be related to an observable and measurable crack length. Both linear and nonlinear damage rules for the accumulation of fatigue damage have been proposed. Only the linear damage rule will be discussed here.

The most commonly applied linear damage rule was originally proposed in 1924 and was developed further by Miner.[17] The method is referred to simply as *Miner's rule.* Damage under cyclic loading is defined as the ratio of the number of applied cycles, n_i, at stress level σ_i to the number of cycles to failure, N_i, in a constant-amplitude test conducted at σ_i. The hypothesis states that failure occurs when the accumulated damage reaches 1. Mathematically,

$$\Sigma \frac{n_i}{N_i} = \frac{n_1}{N_1} + \frac{n_2}{N_2} + \frac{n_3}{N_3} + \cdots \geq 0 \tag{34.12}$$

This linear damage rule is easily applied after an appropriate counting method has been established. It has the shortcoming, however, that it does not consider the sequence of loading and assumes that damage in any individual stress cycle is independent of what has preceded it. Furthermore, it assumes that damage accumulation is independent of stress amplitude.

CYCLE COUNTING

Some method of cycle counting is required in order to determine the number of cycles at a specific stress range. The tabulation of stress cycles at the various stress ranges is referred to as the stress spectrum. Several counting methods have been proposed, and a summary of these methods is contained in Ref. 18. The two counting methods most commonly used are the *rainflow counting method* and the *reservoir method.* The following example from Ref. 19 demonstrates the procedures.

The rainflow counting method employs the analogy of raindrops flowing down a pagoda roof. Peaks and troughs for one loading event are presented in Fig. 34.9*A*. The maximum and minimum stresses are indexed in Fig. 34.9*B*. The following rules apply to rainflow counting:

1. A drop flows left from the upper side of a peak or right from the upper side of a trough and onto subsequent "roofs" unless the surface receiving the drop is formed by a peak that is more positive for left flow or a trough that is more negative for right flow. For example, a drop flows left from point 1 off points 2, 4, and 12 until it stops at the end of the loading event at point 22, since no peak is encountered that is more positive than point 1. On the other hand, a drop flows right from point 2 off point 3 and stops, since it encounters a surface formed by a trough (point 4) that is more negative than point 2.

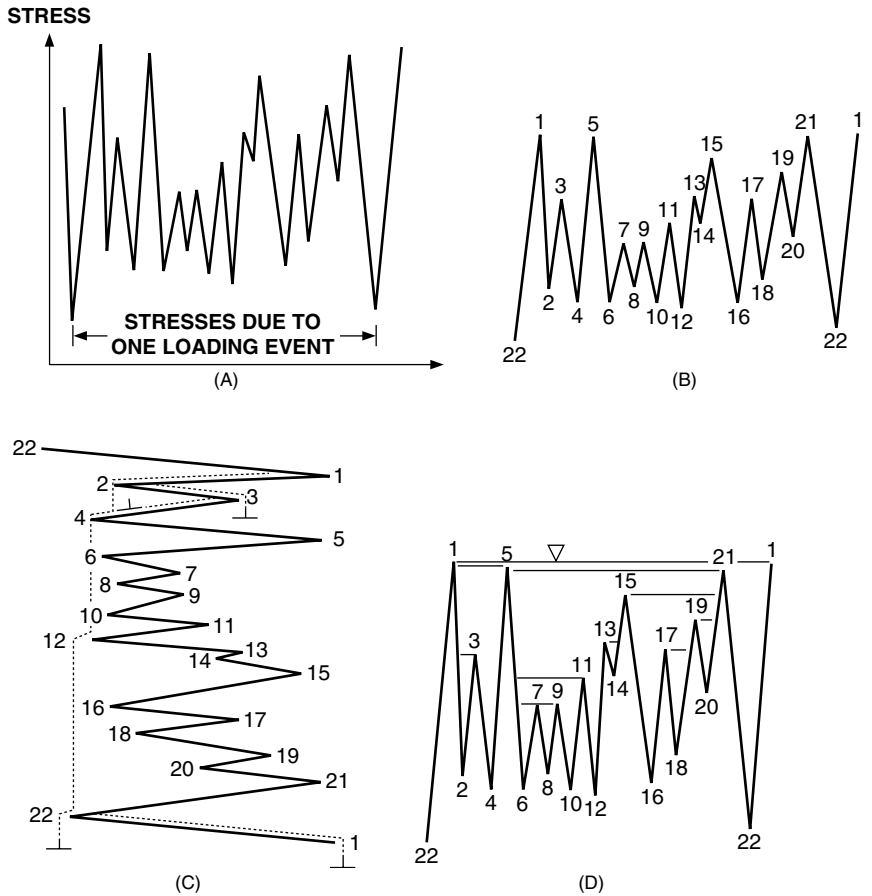

FIGURE 34.9 Variable-amplitude loading for analysis. (*A*) An example of stress variation in an element due to one loading event. (*B*) Peaks and troughs numbered for one loading event. (*C*) Rainflow analysis. (*D*) Reservoir analysis.

2. The path of a drop cannot cross the path of a drop that has fallen from above. For example, a drop flowing left from point 3 stops at the horizontal position of point 2 because it encounters a path coming from point 2.

3. The horizontal movement of a raindrop, measured in units of stress from its originating peak to its stop position, is counted as one-half of a cycle in the stress spectrum.

The stress variation of Fig. 34.9*A* is rotated 90° in Fig. 34.9*C* for application of the rainflow counting method. The values of the peaks for the stress history shown in Fig. 34.9 are given in Table 34.9. Table 34.10 contains the values of the half-cycle magnitudes which result from application of the rules above.

TABLE 34.9 Stress Values for Fig. 34.9

Peak/trough no.	Stress, MPa
1	93
2	18
3	55
4	10
5	85
6	10
7	37
8	18
9	37
10	10
11	46
12	6
13	55
14	46
15	74
16	8
17	55
18	18
19	65
20	39
21	83
22	0

TABLE 34.10 Rainflow Counting

From peak or trough no.	To horizontal distance of point no.	Half cycle, MPa
1	22	93
2	3	37
3	2	37
4	5	75
5	6	75
6	11	36
7	10	27
8	9	19
9	8	19
10	9	27
11	10	36
12	21	77
13	14	9
14	13	9
15	16	66
16	15	66
17	18	37
18	17	37
19	20	26
20	19	26
21	12	77
22	1	93

The reservoir method employs an analogy of water contained in reservoirs formed by peaks draining successively out of the troughs. The lowest trough is drained first, followed by successively higher troughs until the reservoir is empty. Figure 34.9*D* demonstrates the reservoir method, and the corresponding values for the stress range are presented in Table 34.11.

TABLE 34.11 Reservoir Counting Method

Drain from trough no.	Water level at peak	Stress range, MPa
22	1	93
12	21	77
4	5	75
16	15	66
2	3	37
18	17	37
10	11	36
6	7	27
20	19	26
8	9	19
14	13	9

Rainflow counting and reservoir counting give identical results provided that rainflow counting begins with the highest peak in the loading event, as is shown in Fig. 34.9. Rainflow counting is more suited to computer analyses or long stress histories, whereas the reservoir method is most convenient for graphical analyses of short histories.

Table 34.12 presents the results of an analysis according to the Miner linear damage rule assuming 1 million loading sequences of the stress history of Fig. 34.9. The cyclic fatigue lives presented in the second column are taken from a typical *S-N* curve for a beam in which manually welded longitudinal fillet welds are used to connect the flanges to the web. The analysis indicates that the fatigue evaluation has failed.

TABLE 34.12 Cumulative Damage Using Miner's Rule

Stress range, $\Delta\sigma$, MPa	Fatigue resistance, $N = (100/\Delta\sigma)^3, 2 \times 10^6$ cycles	Damage due to 1×10^6 loading events, n_i/N
93	2,490,000	0.402
77	4,381,000	0.228
75	4,741,000	0.211
66	6,957,000	0.144
37 (twice)	39,480,000	0.051
36	42,870,000	0.023
27	101,600,000	0.010
26	113,800,000	0.009
19	292,600,000	0.003
9	2.7×10^9	0.000
		Damage summation: $\Sigma n_i/N = 1.08 \geq 1.0$

The cyclic fatigue lives in Table 34.12 do not reflect the existence of an endurance limit or constant-amplitude fatigue limit. Because the Miner rule does not account for the effect of load sequence, some designers choose to extend the finite life region of the *S-N* curve and assume that all cyclic variations contribute to damage accumulation. The opposite extreme would be to neglect all cyclic variations smaller than the constant-amplitude fatigue limit. A third variation of the procedure employed by some designers assumes a change in the slope of the experimentally determined *S-N* curve at some large number of cycles. For example, between 5×10^6 cycles and 10^8 cycles the slope of the *S-N* curve might be reduced, and the constant-amplitude fatigue limit might be assumed to occur at 10^8 cycles. In view of the lack of test data at very long fatigue lives, there is no agreement on which of the three procedures is most appropriate.

REFERENCES

1. Obtainable from the American Society for Testing and Materials, 1916 Race Street, Philadelphia, PA 19103.
2. Vallance, A., and V. Doughtie: "Design of Machine Members," 3d ed., chap. II, McGraw-Hill Book Company, Inc., New York, 1951.
3. Hoyt, S. I.: "Metal Data," 2d ed., Reinhold Publishing Corporation, New York, 1952.
4. American Society for Metals: "Metals Handbook," Vol. 1, "Properties and Selection: Irons, Steels, and High-Performance Alloys," 1990.
5. Clark, D. S., and D. S. Wood: *Trans. ASM,* **42:**45, 1950.
6. Manjoine, M. J.: *J. Appl. Mechanics,* **66:**A215, 1944.
7. MacGregor, C. W., and J. C. Fisher: *J. Appl. Mechanics,* **67:**A217, 1945.
8. Lessells, J. M.: "Strength and Resistance of Metals," p. 7, John Wiley & Sons, Inc., New York, 1954.
9. Battelle Memorial Institute: "Prevention of Failure of Metals under Repeated Stress," John Wiley & Sons, Inc., New York, 1946.
10. Bannantine, J. A., J. J. Comer, and J. L. Handrock: "Fundamentals of Metal Fatigue Analysis," Prentice-Hall, Inc., Englewood Cliffs, N.J., 1990.
11. Barsom, J. M., and S. T. Rolfe: "Fracture and Fatigue Control in Structures," 2d ed., Prentice-Hall, Inc., Englewood Cliffs, N.J., 1987.
12. American Institute of Steel Construction: "Specification for Structural Steel Buildings—Allowable Stress Design and Plastic Design," 1989.
13. American Railway Engineering Association: "Specifications for Steel Railway Bridges," 1994.
14. American Association of State Highway and Transportation Officials: "Standard Specifications for Highway Bridges," 1992.
15. American Welding Society: "Structural Welding Code," D1.1, 1994.
16. Gaylord, E. H., Jr., C. N. Gaylord, and J. E. Stallmeyer: "Structural Engineering Handbook," 4th ed., The McGraw-Hill Companies, Inc., New York, 1996.
17. Miner, M. A.: *J. Appl. Mech.,* **12:**A159 (1945).
18. Gurney, T. R.: "Fatigue of Welded Structures," 2d ed., Cambridge University Press, 1979.
19. Kulak, G. L., and I. F. C. Smith: "Analysis and Design of Fabricated Steel Structures for Fatigue: A Primer for Civil Engineers," *Structural Engineering Report* No. 190, University of Alberta, Edmonton, Canada, 1993.